Electron-impact dissociation of oxygen

P. C. Cosby
Molecular Physics Laboratory, SRI International, Menlo Park, California 94025

(Received 3 February 1993; accepted 12 March 1993)

The electron-impact dissociation of O_2 to form two oxygen atoms is observed in a crossed beam experiment at electron energies between 13.5 and 198.5 eV. Detection of the correlated dissociation fragments with a time and position sensitive detector permits detection of both ground and excited state fragments, but excludes interference from dissociative ionization products. The observed translational energy releases in the O_2 dissociation are consistent with production of $O(^1D)+O(^3P)$ fragments following electron impact excitation to the $B\,^3\Sigma_u^-$, $B'\,^3\Sigma_u^-$, and $2\,^3\Pi_u$ states, and production of $O(^3P)+O(^3P)$ fragments from excitation to the (unresolved) $c\,^1\Sigma_u^-$, $A'\,^3\Delta_u$, and $A\,^3\Sigma_u^+$ states. Absolute cross sections for the electron impact dissociation of O_2 are measured.

INTRODUCTION

The O_2 molecule is an important constituent of the atmosphere and other gaseous media. The importance of obtaining an understanding of its response to electron impact, such as occurs in aurora and discharges, has prompted a large number of experimental and theoretical investigations of this species. Total electron impact cross sections are well known as are those for ionization, elastic scattering, rotational and vibrational excitation, and for the excitation to several of the electronic states in this species. However, dissociation cross sections must be inferred from the cross sections measured for excitation to specific electronic states. Compilations of cross sections for electron impact processes in O_2 are available from several sources.[1–3]

The O_2 molecule provides perhaps the best case for inferring dissociation cross sections from excitation cross sections since all of its electronic states that are accessible from a thermal population in the ground $X\,^3\Sigma_g^-$ state with electric dipole allowed transitions lie above the first dissociation limit and appear to dissociate. Optical emission in the Schumann–Runge bands is observed in O_2 discharges at high pressure,[4] but the fraction of emitted light is small because all levels of the upper state of this system, $B\,^3\Sigma_u^-$, are found to rapidly predissociate.[5–7] At lower pressures, only optical emission from highly excited atomic O, O^+, and O^{++} states is observed[8–10] and highly excited neutral fragments formed by electron impact on O_2 have been detected using nonoptical techniques.[11–13] In general, the processes forming highly excited fragments represent only a small subset of the overall O_2 dissociation, and frequently their formation is through dissociation processes in the O_2^+ ion.

Direct detection of the dominant O_2 dissociation fragments has historically been difficult. Formation of O atom products in the ground ^3P state and in the lower excited states, ^1D and ^1S, accounts for all of the accessible dissociation limits below the ionization limit of the molecule. The ^1D and ^1S excited states are long lived, with radiative lifetimes of 148 and 0.8 s, respectively. These excited states can be monitored by their red and green line emission in the upper atmosphere, but are subject to rapid collisional quenching or reaction in most laboratory environments. Nevertheless a few laboratory measurements of ^1S, ^1D, and ^3P production following photodissociation of O_2 have been made.[14–17] In addition, there has been one unpublished measurement using chemi-ionization to detect O atom production following electron impact dissociation of O_2.[18]

The approach in the present experiment is to study the reaction

$$O_2+e\rightarrow O_2^*+e\rightarrow O+O+e+W \qquad (1)$$

in a crossed beam experiment. The O_2 beam is formed with several keV of translational energy such that the O-atom dissociation fragments can be detected by secondary electron emission at an electron multiplier detector. At high impact velocities, the secondary emission efficiencies of individual atomic states are roughly the same; hence fragments produced at the lower dissociation limits can be detected. The high velocity of the molecules further serves to constrain the spatial dispersion of the fragments such that all of the fragments, or at least a known fraction of them, can be detected. The fragments are detected in multiple coincidence with respect to their spatial and temporal separations, allowing a discrete pair of atomic fragments to be directly associated with the dissociation of a single molecule and to obtain an explicit measurement of the translational energy release W. Charged dissociation products are explicitly excluded from detection; hence products of electron-impact dissociation O_2, reaction (1), are observed without contributions from dissociative ionization processes in the present work.

EXPERIMENT

The experimental apparatus and measurement procedures have been described in detail for the electron-impact dissociation of CO (Ref. 19) and will be considered only briefly here. A fast (3–5 keV), collimated beam of O_2 molecules is created by near-resonant charge transfer neutralization of an O_2^+ beam and intersected at right angles by an electron beam within an interaction region defined by a narrow slit and a beam flag. Undissociated molecules are

 0021-9606/93/129560-10$06.00

collected by the beam flag. If an O_2 molecule dissociates within this region and its fragments are produced with sufficient transverse velocity to escape collection by the beam flag, the correlated pair of fragments is detected by a position sensitive detector (PSD-C) which measures their radial (R) and temporal (Δt) separations.[20] This measurement specifies the center-of-mass translational energy released in the dissociation (W), i.e., the difference in energy between the dissociating molecular state and its atomic products at infinite separation

$$W=\frac{E_0}{4L^2}\left[R^2+\left(\frac{2E_0\Delta t}{M}\right)^2\right]. \quad (2)$$

Here the translational energy of the fast O_2 beam, E_0, is taken to be the energy of the O_2^+ precursor in the charge transfer, M is the mass of O_2, and L is the distance between the point of dissociation of the O_2 molecule and the PSD-C. Both of these are taken to be constants describing all dissociating O_2 molecules. The measurement further specifies the angular distribution of the fragments in the planes orthogonal to the detector. The fast O_2 beam flux is measured by a pyroelectric bolometer and the absolute collection efficiency of PSD-C for dissociation fragments is calibrated. All charged particles are collected by a weak electric field in the region between the beam flag and the PSD-C; hence dissociative ionization products do not contribute to the present measurements.

As described previously,[19] the electron beam has a rectangular geometry and an energy spread of ~ 1.5 eV FWHM. Energy calibration of the electrons is made from the observed threshold for the ionization of Ar (Ref. 21) and has an estimated accuracy of ± 1 eV. Overlap between the electron and neutral beams is controlled by physically translating the electron gun and electron collector as a unit. This capability allows distinction to be made between neutral fragments created by spontaneous or collisional dissociation of the O_2, and electron impact dissociation of O_2. The gun translation further allows an accurate dissociation cross section to be measured without a specific determination of the form factor describing the overlap of the electron and neutral beams.

With the electron gun and the neutral beam aligned, overlap of the beams takes place within a $\Delta L=2.6$ cm interval along the neutral beam flight path. Since it is not known *a priori* where along this interval a particular O_2 molecule dissociates to produce a detected pair of fragments, the value of W implied by Eq. (2) can deviate from the true magnitude of the translational energy release by the factor

$$\frac{\Delta W}{W}=\frac{2\Delta L}{L}=0.052. \quad (3)$$

This factor represents the effective translational energy resolution achieved by the PSD-C for the electron-impact dissociation fragments. Pressures in the interaction region were maintained at $<2\times10^{-8}$ Torr in the present measurements.

Two orientations of the electron beam velocity vector with respect to the PSD-C in combination with the fragment angular distribution observed by the PSD-C are required to define the full angular distribution of the electron-impact dissociation fragments. In the present measurements, these distributions are found to be isotropic within the center-of-mass frame of the O_2 at electron-impact energies >25 eV. At lower electron energies, the flux of fragments dispersed in both energy release and angle was too small for a detailed angular distribution to be determined. In interpreting the present data, we presume that this distribution remains isotropic at lower electron energies.

The internal state distribution of the O_2 beam is determined by the composition in the O_2^+ reactant beam and by the gas used for the neutralization. In order to achieve a substantial difference in populations, the O_2^+ ions used in the present work were created by two different ion sources. A Nier-type source produced O_2^+ by 100 eV electron impact (EI) on O_2 gas. Following the >5 μs transit time between the ion source and the charge transfer neutralization region, the O_2^+(EI) beam consists of ions in two electronic states: $X\,^2\Pi_g$ and $a\,^4\Pi_u$. The vibrational distribution of the ions in these states is explicitly measured by observing with the PSD-C the dissociative charge transfer (DCT) products of O_2^+ following neutralization in Cs vapor. The observed vibrational distribution in the $X\,^2\Pi_g$ state, given in Table I of Walter *et al.*,[22] has 93% of the population distributed among $v=0$–4 of the $X\,^2\Pi_g$ state. The vibrational distribution observed for the $a\,^4\Pi_u$ state agrees with that reported by van der Zande *et al.*[23] and by Grieman *et al.*,[24] with 92% of the $a\,^4\Pi_u$ state population distributed among $v=0$–8. The estimated distribution of population between the X and a states is 0.47 and 0.53, respectively.[22] A second ion source[25] produced O_2^+ with a hollow cathode (HC) discharge in 0.5–1 Torr of O_2 gas. These O_2^+(HC) ions are found to populate only $X\,^2\Pi_g(v=0)$ as evidenced by their Cs DCT translational energy release spectrum.[26]

Charge transfer neutralization from the initial ion state distribution determines the final population distribution in the O_2 beam. The present measurements were made using O_2, furan, or Ar as the neutralizing gas. These have ionization potentials of 12.06, 8.88, and 15.76 eV, respectively. Pressures in the charge transfer cell were adjusted in each case such that the transmitted O_2^+ beam current was attenuated by approximately 10%. Under these conditions, both O_2 and furan produced an O_2 beam with comparable efficiency, but Ar provided a substantially lower neutral beam flux. At keV energies, the product state distribution produced by the charge transfer of a particular initial ion state is determined by both the vibrational overlap integrals in the ionization and recombination steps and the magnitude of the energy defect in the reaction. For the case of O_2^+, these requirements conflict such that the transfer of population between specific vibrational levels in the ion and the neutral is not adiabatic. Partial charge transfer cross sections have been calculated[27] for the production of specific product states in the reaction

$$O_2^+(X,v')+O_2(X,v=0)\rightarrow O_2(X,v'')+O_2^+(X,v^*) \quad (4)$$

at 2210 eV. They predict that even from $v'=0$, significant populations will be created in $v''=0$–2 of the products, with 90% of the product population distributed in $v''\leqslant 4$. This should be an appropriate estimate for the fast O_2 beam population distribution produced by charge transfer in O_2 of 3000 eV $O_2^+(HC)$. A similar distribution is also expected from the calculated cross sections for the neutralization of the $X\,^2\Pi_g$ component of $O_2^+(EI)$, despite the incidence of vibrational excitation in the reactant ion. However, neutralization of the large population of $a\,^4\Pi_u$ state in the $O_2^+(EI)$ beam with O_2 has near-resonant product channels leading to the production of high vibrational levels in O_2, more than 4 eV above the ground vibrational level.[28] There is no reliable way to estimate the O_2 beam state distribution produced by neutralization in furan or Ar. Empirically, it is found here that electron-impact dissociation cross sections measured for the O_2 beam produced from $O_2^+(HC)$ were comparable for each of the three charge transfer gases, suggesting comparable vibrational distributions. In contrast, O_2 beams produced from $O_2^+(EI)$ yielded significantly smaller cross sections, suggesting a higher degree of vibrational excitation.

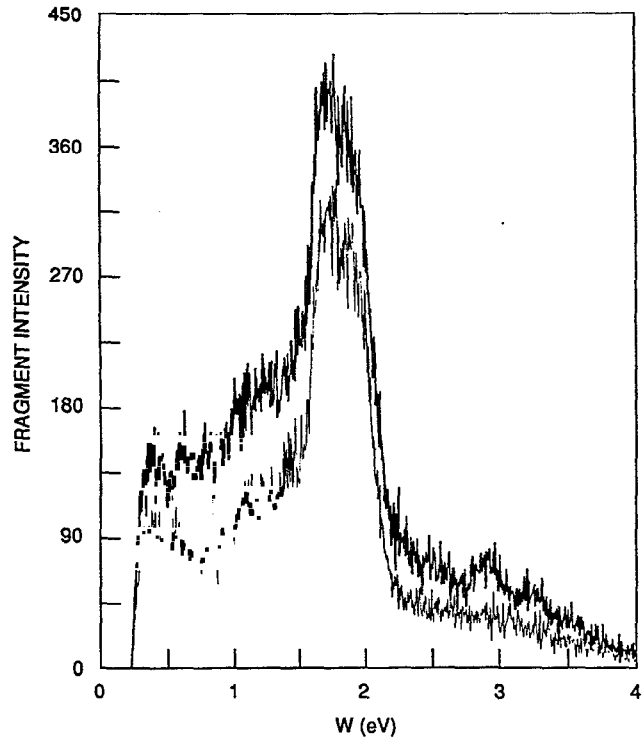

FIG. 1. Distribution of translational energy releases W observed for the dissociation of O_2. The spectra are uncorrected for the variation in the collection efficiency of the apparatus with W. The upper spectrum is obtained with a 48.5 eV electron beam intersecting the fast O_2 beam. The lower spectrum is observed with the electron gun positioned such that the electron beam and O_2 beam do not intersect. These spectra were obtained for O_2 produced by charge-transfer neutralization of $O_2^+(EI)$ to enhance the spontaneous dissociation structure. Direct subtraction of the two spectra gives the translational energy released in the electron-impact dissociation of O_2.

RESULTS

Fragment energy release

The distribution of translational energy releases produced by dissociation of a 3000 eV O_2 beam formed in the charge-transfer neutralization of $O_2^+(EI)$ in O_2 is shown in Fig. 1. The spectra are uncorrected for the collection efficiency of the apparatus, which produces the apparent cut off in the fragment intensity near $W=0.2$ eV and produces some attenuation of the fragment intensity for $W<1$ eV and $W>4$ eV. The upper spectrum in this figure is obtained with a 1.1 mA beam of 50 eV electrons intersecting the O_2 beam with a flux of 5×10^9 s^{-1}, while the lower spectrum is obtained under the same conditions, but with the electron gun repositioned such that there is negligible overlap between the electron and neutral beams. The total accumulation time of the two spectra was 9.7 h with a 50% duty cycle for intersecting and nonintersecting beams. The two spectra are histograms of the apparent value of W implied by Eq. (2) from measured values of R and Δt for each pair of correlated dissociation fragments; fragments observed during beam intersection are binned separately from those observed during nonintersection.

The lower spectrum thus represents the dissociation background to the electron impact dissociation studies and consists of a structured energy releases in the region 1 eV$\leqslant W\leqslant$2.2 eV superimposed on a continuum of energy releases that decreases in intensity with increasing W. Studies of this spectrum as a function of residual gas pressure in the interaction region show an increase in the overall continuum intensity with increasing gas pressure in the range of 10^{-8} to 10^{-7} Torr, suggesting that the continuum arises from collision induced dissociation of the O_2 beam

$$O_2+X\rightarrow O_2^*\rightarrow O+O+W. \tag{5}$$

This continuum contribution was found to be somewhat stronger when furan was used as the neutralizing gas than when O_2 was used.

In contrast, the structured region of the spectrum is effectively unchanged by either gas pressure changes or the choice of O_2 or furan as the neutralizing gas. The energy release near 1.8 eV is more prominent in beams produced from $O_2^+(EI)$ than from $O_2^+(HC)$, but the lower energy features are essentially invariant with the state composition of the O_2^+ beam. These findings suggest that the structured components in the energy release spectrum of the background dissociation arise from dissociative charge transfer of O_2^+

$$O_2^++X\rightarrow O_2^*\rightarrow O+O+W, \tag{6}$$

where the O_2^* produced in the charge transfer must survive transit between the charge transfer cell and the entrance to the interaction region (the slit) before dissociating, a time period of roughly 3 μs. From the broad appearance of the energy releases and the large energy defect ($\sim$7 eV) required for the charge transfer reaction to produce an O_2 state lying >1 eV above the lowest dissociation limit, we estimate that the spectrum arises from a very small concentration ($\sim$1 ppm) of O_2^* in the fast beam with a disso-

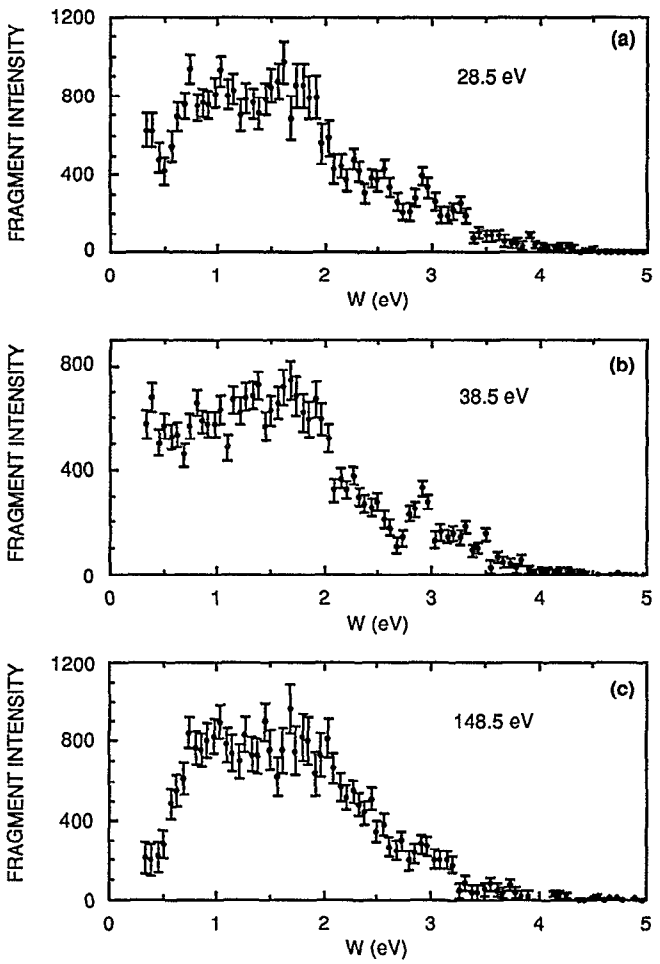

FIG. 2. Translational energy release distributions produced by electron-impact dissociation of O_2 at three electron energies. The distributions have been corrected for collection efficiency, but not for the variation in energy resolution with W [see Eq. (3)].

ciation lifetime of order 10 μs. This is discussed in more detail elsewhere.[29] It should be noted that fragments produced by collisional dissociation or spontaneous dissociation are collected from essentially the entire distance between the slit and the beam flag, not just within the region of electron beam neutral beam overlap. Thus the resolution (and accuracy) of translational energy releases is substantially degraded, with $\Delta W/W \sim 0.34$ for the products of reactions (5) and (6).

The translational energy release spectrum for electron-impact dissociation of O_2, reaction (1), is given by a direct subtraction of the two spectra in Fig. 1. The results of such subtractions, now corrected for PSD-C collection efficiency and binned into fewer channels, are shown in Fig. 2 for electron beam energies of 28.5, 38.5, and 148.5 eV. The spectra, which are not corrected for resolution, Eq. (3), are measured using an O_2 beam produced from $O_2^+(HC)$ neutralized in O_2. The error bars given for the fragment intensity at each W represent the statistical error associated with the subtraction and the calculated collection efficiency. Over most of the spectrum, the collection efficiency is quite flat (see Fig. 6 of Ref. 19). However, at $W < 0.5$ eV, the true collection efficiency is strongly dependent on the precise alignment of the beam flag with the O_2 beam; hence the actual uncertainties in this region can be significantly larger than implied by the error bars. Detailed W spectra of the dissociation fragments were obtained over the electron energy range of 20–200 eV. Below 20 eV, the combination of small dissociation cross sections and small electron beam currents produced W spectra with statistical errors comparable to the binned fragment intensity and were of no utility.

The fragment energy release spectra shown in Fig. 2 exhibit several characteristics. At all electron energies, most of the O_2 dissociations produce a value of W in the range $1 \leqslant W \leqslant 2.5$ eV. We identify this as W region II for later discussion. At electron energies < 70 eV, a significant number of fragments are also produced with $W < 1$ eV. The precise variation of fragment intensity with W is this region is somewhat uncertain, as mentioned above. However, it is quite clear, as shown in Fig. 2, that the number of fragments produced within this region is much smaller for higher electron energies. We designate this as region I. Finally, fragments are produced in the region $2.5 \leqslant W \leqslant 4$ eV, designated as region III. These are somewhat more prominent at the lower electron impact energies. At all electron energies, negligible fragmentation is observed with $W > 4$ eV.

Total dissociation cross section

The total dissociation cross section σ_{dis} is obtained from the relation

$$\sigma_{dis} = \frac{N^* u v_n \eta e}{\xi \chi I_e I_{fc}}, \qquad (7)$$

as discussed in Ref. 19. Here, I_{fc}/η is the O_2 beam flux, I_e is the electron beam current, v_n is the velocity of the O_2 beam, taken here to be the velocity of the O_2^+ precursor, e is the electron charge, ξ is the coincidence efficiency of the PSD-C, and χ is the collection efficiency of the PSD-C, i.e., the fraction of the total cm distribution of the dissociation fragments that is viewed by the detector, N^* is the total accumulated number of electron impact dissociation pairs as the electron beam is slowly translated completely across the O_2 beam at a constant velocity u. Each of these terms is separately measured with the exception of the PSD-C collection efficiency χ, which is an explicit function of the O_2 beam energy, fragment energy release W, and the center of mass angles Θ and Φ defining the ejection of the fragments orthogonal to the plane of the PSD-C and within the plane of the PSD-C, respectively. Only Θ is explicitly measured by the PSD-C for each dissociation event, whereas the Φ distribution must be inferred from a comparison of the total apparent cross sections measured at two different orientations of the electron beam with respect to the active axis of the PSD-C. Thus χ makes the single largest contribution to the uncertainty in σ_{dis}. Finally, an error is introduced into the cross sections by the present inability to observed fragments produced with $W < 0.3$ eV. As can be seen in Fig. 2, there is appreciable fragment flux at values

TABLE I. Cross sections measured for the electron impact dissociation of O_2. Units are 1 Mb$=1\times10^{-18}$ cm^2. Partial dissociation cross sections for the production of fragments with translational energy releases $W>2.7$ eV are also given.

	Total dissociation cross section			Partial dissociation cross section	
Electron energy (eV)	(Mb)	Relative uncertainty (Mb)	Absolute uncertainty (Mb)	$W>2.7$ eV (Mb)	Absolute uncertainty (Mb)
13.5	22.0	9.7	12.2		
18.5	52.9	5.3	18.8		
21.0	56.5	8.7	21.1		
23.5	52.5	5.0	18.5		
28.5	58.7	5.2	20.6	4.9	1.7
33.5	66.3	7.7	23.8	5.6	2.0
38.5	61.0	3.4	21.0	5.2	1.8
48.5	53.4	2.9	18.4	4.6	1.6
58.5	44.4	4.5	15.8	3.9	1.4
73.5	36.6	4.2	13.1	3.2	1.4
98.5	33.1	5.6	13.6	3.0	1.2
148.5	29.6	5.0	11.2	2.8	1.1
198.5	29.1	4.4	10.8	2.9	1.1

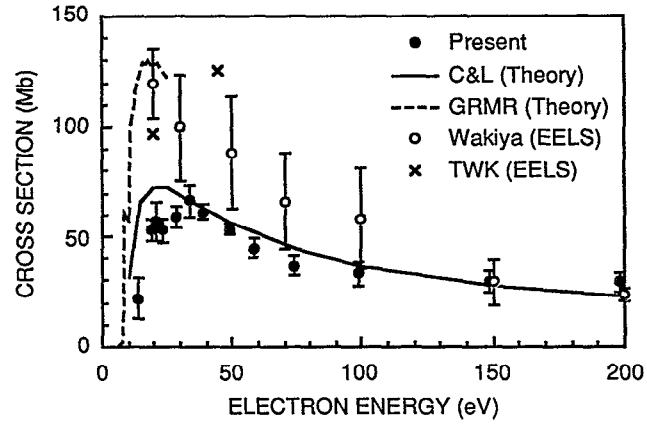

FIG. 3. Dissociation cross sections and excitation cross sections for electron impact on O_2. The present measurements of the total dissociation cross section are given as a function of electron energy by the solid points with error bars reflecting the relative uncertainties of the individual measurements. The solid line labeled CL and the dashed line labeled GRMR are calculations of excitation cross sections to dissociative states by Refs. 54 and 55, respectively. The crosses labeled TWK and open circles labeled Wakiya are experimental estimates of the excitation cross sections to dissociative states in O_2 using electron energy loss spectroscopy by Refs. 35 and 53, respectively, where the error bars represent the absolute uncertainties of Ref. 53.

of W just above this limit, particularly at the lower electron impact energies. However, as discussed in the next section, there is no reason to believe that very low energy releases would dominate the electron-impact dissociation for this molecule. For the present measurements, we approximate this unobserved flux by extrapolating the average fragment intensity observed for the interval $0.3\leqslant W\leqslant 0.5$ eV to $W=0$. This introduces an increase in fragment flux beyond that actually observed ranging from 5% at the higher energies to 14% at the lowest energies. The total absolute uncertainty in the dissociation cross section, taken as the rms sum of the uncertainties in Eq. (7), is ±34%.

Total dissociation cross sections were measured for the O_2 beam produced from O_2^+(HC) neutralized in O_2 or furan and for O_2^+(EI) neutralized in all three charge transfer gases. Cross sections for O_2 formed by the O_2^+(HC) precursor were found to be equal to within ~15% regardless of the neutralizing gas, whereas those for the O_2^+(EI) precursor were systematically ~30% smaller. This difference presumably reflects a higher degree of vibrational excitation in the O_2 produced from O_2^+(EI). The cross sections measured from the O_2^+(HC) precursor are given as a function of electron impact energy in Table I and shown as the solid circles in Fig. 3 in units of 1 Mb$=1\times10^{-18}$ cm^2 $=0.01$ Å^2. The magnitude of the error bars in Fig. 3 reflects only the relative uncertainty in the measured cross sections; the absolute uncertainty is ±34%.

DISCUSSION

Fragment energy release

Representative potential energy curve of O_2 are shown in Fig. 4, which also shows the ground electronic state of O_2^+. Electron impact on O_2 $X\,^3\Sigma_g^-$ produces an electronic excitation in the molecule, as indicated in reaction (1). The O_2 molecule has a great many electronic states, 18 arise from just the lowest dissociation asymptote $^3P+{}^3P$. Considering the possibility of spin-exchange in the collision, excitation of the $X\,^3\Sigma_g^-$ ground state gives access not only to other triplet states as in an electric dipole absorption, but also to the singlet and quintet manifolds as well. A careful consideration of selection rules[30] finds that essentially all of the excited states are accessible to electron impact excitation, though not with equal probabilities.

In the Born approximation, the differential cross section for electron impact excitation is given approximately by[31]

$$\sigma\sim\sigma_0\left[\int_0^\infty \psi_i\psi_f\,dr\right]^2, \tag{8}$$

where σ_0 is the cross section for the excitation of a specific electronic final state from the initial state, here $X\,^3\Sigma_g^-$, for an electron of specific incident and scattered momenta, and the ψ are the wave functions describing the nuclear motion along the internuclear coordinate r in the initial and final electronic states. The term in the right-hand side of Eq. (8) is simply the Franck–Condon factor for excitation between these states. Thus, states accessible to electron impact excitation must lie within a vertical region, shown in Fig. 4 by shading for an initial vibrational level $v=0$. If the final state is a continuum state or a predissociated bound state, the projection of the probability density described by this factor onto the energy coordinate relative to a specific pair of dissociation fragments should closely approximate the distribution of fragments in translational energy release W such as observed in the present experiment.

The lowest excited states of O_2, $a\,^1\Delta_g$ and $b\,^1\Sigma_g^+$ have potential energy curves[32] similar to those of the ground state and thus cannot be excited into a dissociative region

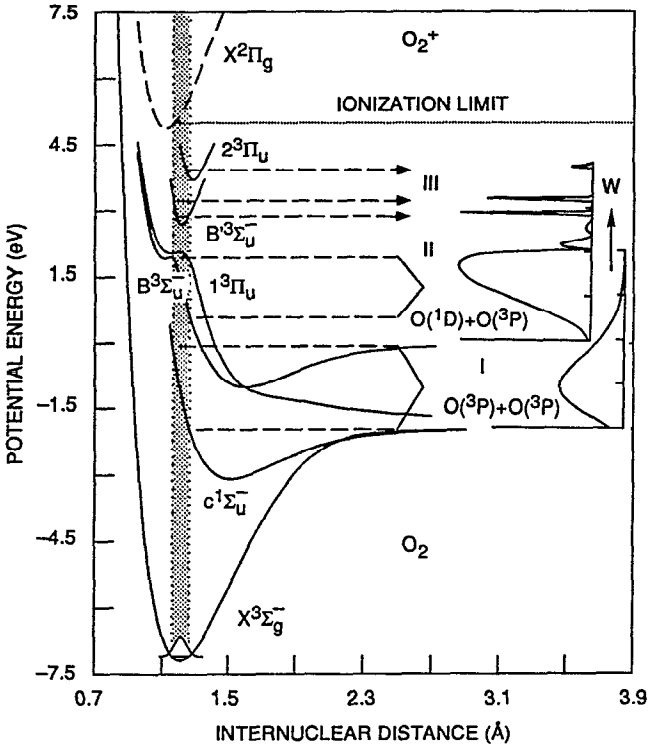

FIG. 4. Potential energy curves of O_2 relevant to electron-impact dissociation. Potential energy is relative to the $O(^1D)+O(^3P)$ separated atoms. The vertical excitation region from O_2 $X\,^3\Sigma_g^-(v=0)$ is indicated by the shaded region. Estimated translational energy release distributions from dissociative states in three regions: I for dissociation to ground state atoms; II and III for production of $O(^1D)+O(^3P)$, are shown to the right of the figure. Tic marks along the energy release distributions are in increments of 1 eV in W. The ground electronic state of O_2^+ and the first ionization limit are also shown in the figure.

with significant probability in a vertical transition, but rather produce only electronic excitation[33–36] upon electron impact. The first dissociative regions accessed in vertical transitions are the repulsive walls of the so-called "6 eV" states, $c\,^1\Sigma_u^-$, $A'\,^3\Delta_u$, and $A\,^3\Sigma_u^+$, which adiabatically dissociate to ground state fragments. The three states have similar potential energy curves[32] and lie close in energy; hence only the $c\,^1\Sigma_u^-$ is shown in the figure. Vertical excitation to the 6 eV states,[34–37] should give rise to production of $O(^3P)+O(^3P)$ with a kinetic energy distribution labeled I, given to the right of the figure, that extends from $W=0$ to $W>2$ eV. The next higher energy dissociation process is to the repulsive wall of the $B\,^3\Sigma_u^-$ state with correlates to $O(^1D)+O(^3P)$ fragments. Excitation in this Schumann–Runge (SR) continuum[38–40] is expected to produce a fragment energy distribution labeled II which is peaked near $W\sim1.7$ eV with a relatively sharp cutoff at higher W due to the avoided crossing of this state in the vertical region with the $^3\Sigma_u^-$ Rydberg state.[41] Also accessible in this region are the repulsive curves arising from the ground state limit, of which the $1\,^3\Pi_u$ is shown in the figure.[39,42] Adiabatic dissociation of these states will produce a form for the W spectrum similar to that of the B state, but shifted to higher kinetic energies by the ^1D–^3P energy separation (1.967 eV). Finally, excitation is possible to Rydberg states formed on the O_2^* $X\,^2\Pi_g$ core.[43] Two of these, the $B'\,^3\Sigma_u^-$ and $2\,^3\Pi_u$ are accessible in dipole allowed transitions from the ground state and are shown in the figure.[44] In addition, the $d\,^1\Pi_g$ and $C\,^3\Pi_g$ Rydbergs lie in the vertical region at a potential energy near 1 eV on the scale of the figure.[45–48] These have been characterized by translational spectroscopy[49] and multiphoton ionization[50,51] studies. All of these states are predissociated. For the B' and $2\,^3\Pi_u$, this is manifested by a substantial broadening of the transitions in the optical absorption spectrum.[52] For the $^{1,3}\Pi_g$, the fragmentation has been explicitly observed to the $^1D+{}^1D$, $^1D+{}^3P$, and $^3P+{}^3P$ dissociation limits.[49] Dissociation products of the $B'\,^3\Sigma_u^-$ and $2\,^3\Pi_u$ states are not known. Dissociation to $^1D+{}^3P$ has been assumed in Fig. 4, as suggested by photodissociation studies,[14,15] giving rise to the discrete energy releases labeled III.

The electron energy dependence of the differential cross section for excitation to the various electronic states in O_2 is given quite precisely by electron energy loss spectroscopy (EELS), which measures the energy and intensity of electrons inelastically scattered from a monochromatic electron beam. The difference in energy between the incident and scattered electrons is equal to the vertical excitation energy between the initial O_2 $X\,^3\Sigma_g^-(v=0)$ state and the final excited state. This differs from the translational energy release W measured here for dissociative states by the energy of the dissociation limit relative to $X\,^3\Sigma_g^-(v=0)$. The O_2 EELS spectrum observed by Wakiya[53] for electrons scattered by 15° following 50 eV electron impact is shown at the bottom of Fig. 5. This spectrum has an energy resolution comparable to that of the translational energy release spectra measured in the present work. A constant value of 7.083 eV has been subtracted from the observed EELS energy losses to place the energy scale of the spectrum in this figure relative to the $O(^1D)+O(^3P)$ dissociation limit, i.e., the zero of potential energy in Fig. 4. At 50 eV electron impact energy, the spectrum is dominated by dipole allowed transitions: excitation of the SR continuum $B\,^3\Sigma_u^-\leftarrow X\,^3\Sigma_g^-$ occurs for energy losses between 0 and 2.2 eV and should produce fragmentation corresponding to region II in Fig. 4, and excitation of the $B'\,^3\Sigma_u^-$ and $2\,^3\Pi_u$ Rydberg states at energy losses near 3 eV, corresponding to region III in Fig. 4. The small undulations at the top of the SR feature have been assigned to excitation of the $^3\Pi_g$ Rydberg state.[40] Excitation to the 6 eV states, region I in Fig. 4, also contribute weakly to the EELS spectrum, but at energies below the energy zero on the scale of Fig. 5. While the relative intensities in the EELS spectrum are those obtained at a 15° scattering angle, they roughly reflect the relative excitation cross sections integrated over all scattering angles.

The fragment translational energy release spectrum obtained in the present work following 48.5 eV electron impact is shown at the top of Fig. 5. The similarity between the fragment energy spectrum and the EELS spectrum is strikingly good, both in terms of the cutoff for the SR feature near 2 eV and the appearance of fragments following predissociation of the $B'\,^3\Sigma_u^-$ and $2\,^3\Pi_u$ Rydberg

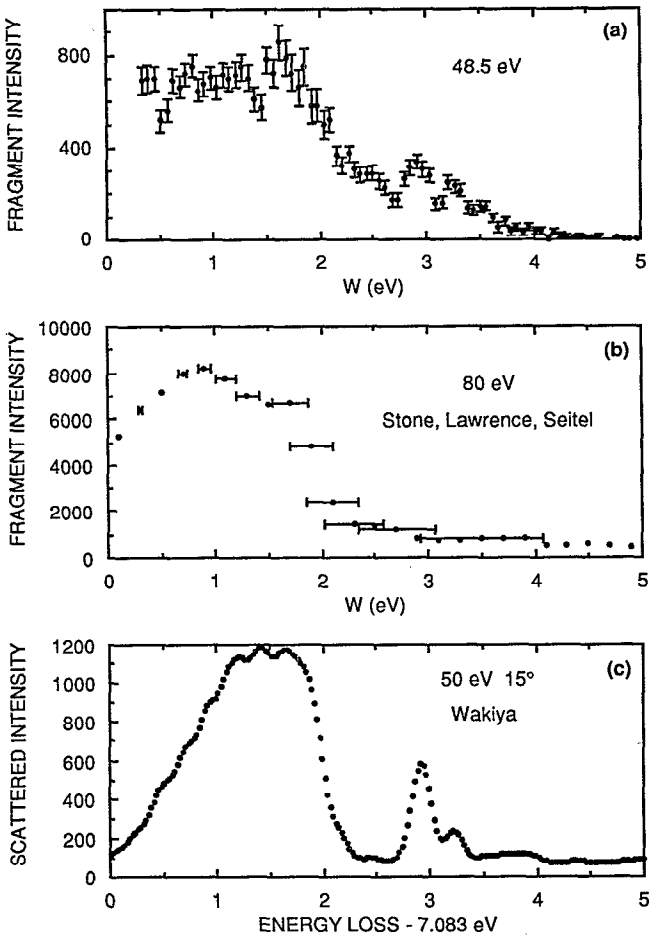

FIG. 5. Three energy distributions of O_2 referenced to a common energy scale. The upper distribution is the translational energy release observed in the present work following 48.5 eV electron impact dissociation of a fast O_2 molecular beam. The center distribution is the translational energy release distribution obtained by transforming the $O(^3P)$ arrival time distribution observed by Ref. 18 following 80 eV electron impact on thermal O_2. The bottom distribution is the scattered electron intensity at 15° as a function of energy loss observed by Ref. 53 following 50 eV electron impact on thermal O_2. A value of 7.083 eV has been subtracted from the observed energy loss to reference it to the $O(^1D)+O(^3P)$ dissociation limit. The ordinates of each distribution are linear, but the numerical labels are arbitrary.

states. In fact, the appearance of these fragments near 3 eV provides definitive evidence for predissociation of these states to the $^1D + {}^3P$ dissociation limit; their positions in the spectrum would be shifted by ~2 eV to higher or lower energy if other dissociation products were formed. Production of fragments at this limit has also been found following photoexcitation to these states.[14,15]

The main deviation between the fragment and EELS spectra occurs for $W<1$ eV, where there is substantially more intensity than would be suggested by the excitation spectrum. However, excitation of the 6 eV states necessarily must produce ground state fragments. These correspond to region I of Fig. 4 and will contribute to the fragment intensity within the $W<1$ eV region. Further justification for attributing the significant fragment intensity in this region to dissociation of the 6 eV states comes from the electron energy dependence of these fragments shown in Fig. 3. Substantially fewer fragments appear in this region for electron impact energies >70 eV. Waikya[53] has reported integral excitation cross sections for the 6 eV group of states and for the SR continuum at several electron impact energies. The ratio of his cross sections σ_{6eV}/σ_{SR} decrease from 0.105 at 20 eV to 0.021 at 100 eV. The relative decrease in the excitation cross section is consistent with the relative decrease in low W fragment intensity with increasing electron impact energy.

A second disagreement between the excitation spectrum and the fragment spectrum is the relatively high fragment flux in the region 2.2 eV$\leqslant W \leqslant$2.7 eV between the high energy side of the SR feature and the B' fragments. An obvious source for such fragments would be from SR continuum dissociation accessed from vibrationally excited O_2 molecules in the fast beam. The EELS spectrum was obtained with an O_2 target gas equilibrated at room temperature; hence essentially all molecules are in the $v=0$ initial state. In contrast, we expect a distribution of vibrational levels, $0\leqslant v\leqslant 4$ to be populated in the fast O_2 beam by charge transfer. However, if the effect of such vibrational excitation on the bound–free Franck–Condon factors is explicitly modeled using the empirical potential energy curves of Allison *et al.*,[42] it is found to produce relatively little broadening in the fragment energy release spectrum. Although vibrational excitation expands the range of internuclear distances over which vertical excitation can take place, the main effect of this is to increase the relative fragment flux from dissociation in the SR continuum near $W\sim 1.8$ eV, rather than to substantially broaden the feature to higher values of W. This is due to the inflection in the B state potential curve from an avoided crossing; its form has been empirically defined by Allison *et al.* to reproduce the optical absorption spectrum. In fact, there is some evidence of a weak peak in the fragment spectrum near 1.8 eV, which may be the manifestation of O_2 vibrational excitation. Another effect of vibrational excitation may be to weaken the features at $W\sim 3$ eV attributed to B', $2\,{}^3\Pi_u$ predissociation relative to the SR feature at $W\sim 1.7$ eV. However, the energy releases of the predissociation features cannot be broadened by vibrational excitation. It therefore seems likely that the fragments in the region above the expected SR cutoff arise from dissociation of the 6 eV states, which are expected to produce fragments in excess of $W=2.2$ eV even from an initial $v=0$ state, as indicated by distribution I in Fig. 4.

Another measure of the effects of O_2 vibrational excitation comes from the work of Stone, Lawrence, and Seitel.[18] These authors reported the time of flight spectrum of O atom fragments produced following the dissociation of thermal O_2 molecules with a pulsed, 80 eV electron beam. Chemi-ionization of the O atoms in a samarium vapor cell allowed detection of ground state atoms.[14] Their time-of-flight spectrum, now transformed onto an energy release scale, is shown at the center of Fig. 5. Horizontal error bars given in the figure indicate the rapid degradation in energy resolution with increasing energy release that accompanies a constant uncertainty in fragment flight time. In general,

the fragment energy distribution compares favorably to that observed at $W<1$ eV in the present measurements for electron impact energies between 48.5 and 98.5 eV. This gives support to attributing much of the fragment intensity in this region to dissociation of the 6 eV states, rather than to the effects of vibrational excitation. Their spectrum appears to decrease faster in intensity for $W>2$ eV than the present measurements, however it is not clear that this can be attributed to the absence of vibrational excitation of O_2X in their measurements or to the decrease in peak fragment intensity that must accompany the degradation in energy resolution. This latter effect is most certainly responsible for the lack of any discernible feature in their spectrum near $W=3$ eV from Rydberg state predissociation.

Total dissociation cross section

There have been two theoretical calculations of the cross sections for electron-impact dissociation of O_2. Chung and Lin[54] used the Born–Ochkur approximation to calculate the contribution to the electron-impact dissociation cross section arising from $B\,^3\Sigma_u^- \leftarrow X\,^3\Sigma_g^-$ excitation at electron energies between 10 and 1000 eV. Their results are given as the solid line in Fig. 3. The calculations compare quite well with the measured cross sections, certainly within the absolute uncertainty of the measurements. However, only dissociation through the Schumann–Runge continuum has been considered in the calculations; hence they represent only a lower limit to the total dissociation cross section.

Calculations of the electron impact cross section over the electron impact energy range from threshold to 25 eV have been reported by Garrett *et al.*[55] using an impact parameter approach. These calculations considered only excitation in dipole-allowed transitions to the $B\,^3\Sigma_u^-$, $B'\,^3\Sigma_u^-$, and $1\,^3\Pi_u$ states, shown in Fig. 4. The sum of these calculated cross sections as a function of electron energy are given by the dashed line in Fig. 3. Since excitation of the 6 eV states, in particular, has been neglected, the calculated cross section also represents a lower limit to the total dissociation cross section. Nevertheless, the calculated cross section is substantially larger than the present measurements.

Experimental cross sections for electron-impact excitation to several dissociated states of O_2 have also been reported. These have been derived from differential EELS cross section measurements that have been converted to integral inelastic scattering cross sections and normalized to absolute elastic scattering cross section measurements. Trajmar, Williams, and Kuppermann[35] report the excitation cross sections at two electron impact energies to the 6 eV states, the SR continuum, and to the B',$2\,^3\Pi_u$ Rydberg states. The sum of these cross sections are given by the two crosses in Fig. 3. Wakiya[53] has reported the cross sections for excitation to these same states at five electron energies between 20 and 100 eV. The sum of his cross sections are given by the open circles in this figure, together with error bars indicating his estimated uncertainties. The open circles given at electron energies of 150 and 200 eV are Wakiya's cross sections for excitation to the SR continuum alone; it accounts for 85% of the summed cross section at 100 eV and should provide an even closer approximation to the total cross section at these higher energies. There is some disagreement between the two sets of measurements as to the electron energy dependence of the cross section between 20 and 50 eV, but in general the overall magnitudes of the cross section in this region is consistent. There appears to be strikingly good agreement between the Wakiya measurements and the total cross section calculated by Garrett *et al.* However, some of this agreement is fortuitous. Excitation to the B' state contributes 35% of the calculated total cross section at 20 eV, whereas excitation to the B' and higher states contributes only 13% to the total cross section of Wakiya[53] and 15% to the total cross section of Trajmar *et al.*[35]

A comparison between the present cross sections, the solid circles in Fig. 3, and the experimental excitation cross sections from EELS finds the excitation cross sections to be uniformly larger than the present dissociation measurements over most of the electron energy range. Nevertheless, both sets of measurements overlap within their mutual uncertainties for electron energies >25 eV, but at lower energies the disagreement is significant. There is the possibility that some fraction of the states excited in the EELS experiments do not dissociate, however this is unlikely given the present knowledge of the excited states in O_2. A more likely reason for the smaller dissociation cross sections is that they are measured for O_2 with a vibrational population distributed among $v=0$–4. Garrett *et al.*[55] have calculated the effects of vibrational excitation on the excitation cross sections. They find that the cross section for $B\leftarrow X(v)$ at 20 eV decreases by roughly 18% between $v=0$ and $v=2$ and will presumably decrease further for excitation from higher vibrational levels. A decrease in the dissociation cross section with the enhanced vibrational excitation that is produced in the O_2 beam formed from O_2^+(EI) neutralized in O_2 is also found in the present measurements.

Kanik *et al.*[56] have recently compiled a set of recommended electron scattering cross sections for O_2. By subtracting measured values of the cross sections for elastic scattering and ionization from the total scattering cross section, they obtain a measure of the total cross section for the sum of electronic and vibrational excitation over the electron energy range from 1 to 400 eV. Of particular interest here is that this implied excitation cross section has a maximum value at 30 eV of 249 Mb, of which <4 Mb can reasonably be attributed[1–3] to vibrational excitation. However, this implied electronic excitation cross section is nearly a factor of 2 greater than even the largest estimates for the excitation cross sections given in Fig. 3 and a factor of 4 greater than the present measurement of the dissociation cross section. The difference could imply a substantial reservoir for electron-impact excitation other than dissociation, although this seems unlikely given the present knowledge of this molecule. It is more likely that the disagreement reflects the true magnitudes of absolute uncer-

tainty in the electron scattering, ionization, and dissociation cross sections of O_2.

Partial dissociation cross sections

The fragment translational energy release spectra measured in the present work allow some resolution of the total dissociation cross sections into partial cross sections. Determining the relative contributions of the 6 eV states and the SR continuum to the dissociation requires an assumption as to the explicit form of in individual energy release contributions from these two sources of fragments; hence we avoid making such a determination here. On the other hand, there is a fairly clear distinction between the fragments arising from the B',$2\,^3\Pi_u$ and higher Rydberg states and those from the lower energy states. If we attribute the fragment flux with $W>2.7$ eV to dissociation from these higher states, their implied dissociation cross sections are those given in Table I. It can be seen that they range from 6.3 Mb at electron energies near 30 eV to 2.5 Mb near 100 eV. The ratio of these partial cross sections to those reported by Wakiya[53] is roughly 0.4 over this energy range. This ratio is even smaller than the ratio of the total cross sections, 0.58. The smaller ratio may indicate that product channels other than $O(^1D)+O(^3P)$ are also populated in the predissociation, e.g., $O(^1D)+O(^1D)$ or $O(^1S)+O(^3P)$ which could be obscured in translational energy release spectrum by direct dissociation products (fragments I and II in Fig. 4). On the other hand, the smaller ratio may merely reflect a greater sensitivity of these bound–bound transitions to vibrational excitation in the initial state.

The calculations of Garrett *et al.*[55] yield a large cross section for excitation into the B' state, 46 Mb at 20 eV. This value far exceeds the experimental estimates of Wakiya[53] (<15.7 Mb) and of Trajmar *et al.*[35] (1.5 Mb) as well as that obtained from an extrapolation of the present estimates for the partial dissociation cross section to this lower electron energy. Garrett *et al.* assume that tunneling represents the only dissociation path in the B' state and conclude that radiation rather than dissociation will be the dominant decay process in its lowest vibrational levels. This conclusion contrasts sharply with both the present measurements and with previous photoexcitation studies.[14,15] Detailed studies of the absorption bands to the three vibrational levels of the B' state find asymmetric rotational lineshapes with a half-width at half-maximum $>5.6\ cm^{-1}$ in these levels,[52] implying a rapid predissociation of all levels.[52] The discrepancy between the calculations of Garrett *et al.* and experimental observations seems to arise from the use of a purely adiabatic description of the B' state. Recent calculations[57] find that the diabatic character of this state, formed from an avoided crossing of valence and Rydberg $^3\Sigma_u^-$ states, must be explicitly considered to be consistent with optical absorption measurements.

CONCLUSIONS

Absolute dissociation cross sections and translational energy release spectra are measured for electron impact on O_2 in a fast molecular beam. The translational energy release distributions are found to be consistent with the major contributions to O_2 dissociation arising from optically allowed electronic excitation to the $B\,^3\Sigma_u^-$, $B'\,^3\Sigma_u^-$, and $2\,^3\Pi_u$ states, each dissociating to form $O(^1D)+O(^3P)$ atoms. Additional contributions appear in the fragment distributions that are consistent with dissociation of the 6 eV states, $c\,^1\Sigma_u^-$, $A'\,^3\Delta_u$, and $A\,^3\Sigma_u^+$, to $O(^3P)+O(^3P)$ atoms. Production of energy releases $W>4$ eV was found to be negligible at all electron impact energies, suggesting that O_2 states formed at or above the lowest ionization limit either autoionize or dissociate to $O(^1S)+O(^3P)$ or higher limits.

The total dissociation cross section is found to maximize at a value of 66 Mb for electron energies near 33 eV. However, the cross section refers to excitation from a vibrationally excited distribution $X\,^3\Sigma_g^-(v=0\text{–}4)$ in the fast molecular beam. Such excitation is endemic to the fast O_2 beam production via resonant or near-resonant charge transfer neutralization of O_2^+ due to the displacement in equilibrium internuclear separations of the ion and neutral ground electronic states. Tests using an O_2 beam with yet higher vibrational excitation yielded a cross section 30% smaller than this value. The measured dissociation cross section is smaller than previous measurements of the excitation cross sections to the primary dissociating excited states in O_2. While there are substantial uncertainties in *both* the dissociation and the excitation cross sections, it seems most likely that the smaller dissociation cross section can be attributed to this vibrational excitation.

ACKNOWLEDGMENTS

This research was supported by the U.S. Air Force Wright Laboratory under Contract No. F33615-85-R-2560. The author wishes to thank H. Helm and J. R. Peterson for a variety of assistance during the course of this work.

[1] A. V. Phelps, JILA Information Center Report No. 28 (1985).
[2] B. Eliasson and U. Kogelschatz, J. Phys. B **19**, 1241 (1986); *Basic Data for Modelling of Electrical Discharges in Gases: Oxygen*, Brown Boveri Research Report KLR 86-11C (Baden, Switzerland, Brown Boveri Research Center, 1986).
[3] Y. Itikawa, A. Ichimura, K. Ondaz, K. Sakimoto, K. Takayanagi, Y. Hatano, M. Hayashi, H. Nishimura, and S. Tsurubuchi, J. Phys. Chem. Ref. Data **18**, 23 (1989).
[4] D. M. Creek and R. W. Nicholls, Proc. R. Soc. London, Ser. A **341**, 517 (1975).
[5] B. R. Lewis, L. Berzins, J. H. Carver, and S. T. Gibson, J. Quant. Spectrosc. Radiat. Transfer **36**, 187 (1986).
[6] A. S.-C. Cheung, K. Yoshino, J. R. Esmond, S. S.-L. Chiu, D. E. Freeman, and W. H. Parkinson, J. Chem. Phys. **92**, 842 (1990).
[7] P. C. Cosby, H. Park, R. A. Copeland, and T. G. Slanger, J. Chem. Phys. **98**, 5117 (1993).
[8] M. J. Mumma and E. C. Zipf, J. Chem. Phys. **55**, 1661 (1971).
[9] J. M. Ajello and B. Franklin, J. Chem. Phys. **82**, 2519 (1985).
[10] M. B. Schulman, F. A. Sharpton, S. Chung, C. C. Lin, and L. W. Anderson, Phys. Rev. A **32**, 2100 (1985).
[11] R. S. Freund, J. Chem. Phys. **54**, 3125 (1971).

[12]S. Ohshima, T. Kondow, T. Fukuyama, and K. Kuchitsu, Chem. Phys. **135**, 267 (1989).
[13]N. J. Mason and W. R. Newell, J. Phys. B **23**, 4641 (1990).
[14]E. J. Stone, G. M. Lawrence, and C. E. Fairchild, J. Chem. Phys. **65**, 5083 (1976).
[15]L. C. Lee, T. G. Slanger, G. Black, and R. L. Sharpless, J. Chem. Phys. **67**, 5602 (1977).
[16]Y. Matsumi and M. Kawasaki, J. Chem. Phys. **93**, 2481 (1990).
[17]Y.-L. Huang and R. J. Gordon, J. Chem. Phys. **94**, 2640 (1991).
[18]E. J. Stone, G. M. Lawrence, and S. C. Seitel, in *Electronic and Atomic Collisions: Abstracts of Papers of the IXth International Conference on the Physics of Electronic and Atomic Collisions*, edited by J. S. Risley and R. Geballe (University of Washington, Seattle, 1975), pp. 816–817.
[19]P. C. Cosby, J. Chem. Phys. **98**, 7804 (1993).
[20]H. Helm and P. C. Cosby, J. Chem. Phys. **86**, 6813 (1987).
[21]R. C. Wetzel, F. A. Baiocchi, T. R. Hayes, and R. S. Freund, Phys. Rev. A **35**, 559 (1987).
[22]C. W. Walter, P. C. Cosby, and J. R. Peterson, J. Chem. Phys. **98**, 2860 (1993).
[23]W. J. van der Zande, W. Koot, J. R. Peterson, and J. Los, Chem. Phys. **126**, 169 (1989).
[24]F. J. Grieman, J. T. Moseley, R. P. Saxon, and P. C. Cosby, Chem. Phys. **51**, 169 (1980).
[25]H. Helm, Phys. Rev. A **38**, 3425 (1988).
[26]W. J. van der Zande (private communication, 1991).
[27]T. F. Moran, M. R. Flannery, and P. C. Cosby, J. Chem. Phys. **61**, 1261 (1974).
[28]P. C. Cosby and H. Helm, J. Chem. Phys. **90**, 1434 (1989).
[29]P. C. Cosby and H. Helm (in preparation).
[30]W. A. Goddard, D. L. Huestis, D. C. Cartwright, and S. Trajmar, Chem. Phys. Lett. **11**, 329 (1971).
[31]E. N. Lassettre and M. E. Krasnow, J. Chem. Phys. **40**, 1248 (1964).
[32]T. G. Slanger and P. C. Cosby, J. Phys. Chem. **92**, 267 (1988).
[33]S. A. Lawton and A. V. Phelps, J. Chem. Phys. **69**, 1055 (1978).
[34]A. Konishi, K. Wakiya, M. Yamamoto, and H. Suzuki, J. Phys. Soc. Jpn. **29**, 526 (1970).
[35]S. Trajmar, W. Williams, and A. Kuppermann, J. Chem. Phys. **56**, 3759 (1972).
[36]K. Wakiya, J. Phys. B **11**, 3931 (1978).
[37]D. Teillet-Billy, L. Malegat, J. P. Gauyacq, R. Abouaf, and C. Benoit, J. Phys. B **22**, 1095 (1989).
[38]J. Geiger and B. Schröder, J. Chem. Phys. **49**, 740 (1968).
[39]D. C. Cartwright, N. A. Fiamengo, W. Williams, and S. Trajmar, J. Phys. B **9**, L419 (1976).
[40]R. H. Huebner, R. J. Celotta, S. R. Mielczarek, and C. E. Kuyatt, J. Chem. Phys. **63**, 241 (1975).
[41]A. C. Allison, S. L. Guberman, and A. Dalgarno, J. Geophys. Res. **91**, 10193 (1986).
[42]A. C. Allison, S. L. Guberman, and A. Dalgarno, J. Geophys. Res. **87**, 923 (1982).
[43]S. Chung, C. C. Lin, and E. T. P. Lee, J. Phys. B **21**, 1155 (1988).
[44]R. J. Buenker, S. D. Peyerimhoff, and M. Peric, Chem. Phys. Lett. **42**, 383 (1976).
[45]S. Trajmar, D. C. Cartwright, and R. I. Hall, J. Chem. Phys. **65**, 5275 (1976).
[46]D. Spence, J. Chem. Phys. **74**, 3898 (1981).
[47]T. A. York and J. Comer, J. Phys. B **16**, 3627 (1983).
[48]R. P. Saxon and B. Liu, J. Chem. Phys. **73**, 876 (1980).
[49]W. J. van der Zande, W. Koot, J. R. Peterson, and J. Los, Chem. Phys. Lett. **140**, 175 (1987).
[50]A. Sur, C. V. Ramana, W. A. Chupka, and S. D. Colson, J. Chem. Phys. **84**, 69 (1986).
[51]A. Sur, R. S. Friedman, and P. J. Miller, J. Chem. Phys. **94**, 1705 (1991).
[52]B. R. Lewis, S. T. Gibson, M. Emami, and J. H. Carver, J. Quant. Spectrosc. Radiat. Transfer **40**, 1 (1988).
[53]K. Wakiya, J. Phys. B **11**, 3913 (1978).
[54]S. Chung and C. C. Lin, Phys. Rev. A **21**, 1075 (1980).
[55]B. C. Garrett, L. T. Redmon, C. W. McCurdy, and M. J. Redmon, Phys. Rev. A **32**, 3366 (1985).
[56]I. Kanik, S. Trajmar, and J. C. Nickel, J. Geophys. Res. (in press).
[57]Y. Li, M. Honigmann, K. Bhanuprakash, G. Hirsch, R. J. Buenker, M. A. Dillon, and M. Kimura, J. Chem. Phys. **96**, 8314 (1992).